

## Finite element analysis of erosive wear for offshore structure

**Z.G. Liu<sup>1\*</sup>, S. Wan<sup>1</sup>, V.B. Nguyen<sup>1</sup>, Y.W. Zhang<sup>1</sup>**

<sup>1</sup> Institute of High Performance Computing, 1 Fusionopolis Way, #16-16 Connexis, 138632, Singapore

\* Corresponding author: liuzh@ihpc.a-star.edu.sg

---

**Abstract** Erosive wear, which is a complex material damage process caused by particle impacting on the surface of equipments, has been a major concern in oil & gas industry. In this work, we employ three-dimensional finite element (FE) method to investigate the erosion process under multiple particle impacts with both spherical and irregular non-spherical particles. We take into account both elastic-plastic material behaviors, which is described by Johnson-Cook visco-plastic model, and material removal, which is governed by the Johnson-Cook failure model. The relationships between the erosion rate and the particle velocity and impact angle are obtained and compared with published data. The implications of the current simulation results are also discussed.

**Keywords** Erosion rate, Solid particle impact, Finite element analysis (FEA), Failure

---

### 1. Introduction

Erosion wear, which arises from solid particle impacting, is one of the major failure modes that cause offshore structure damage. Erosion is found in a wide range of equipments in offshore industry, in which solid particles are entrained into fluid flow in the operating process, such as gas turbine, oil & gas pipeline, drilling platforms, etc [1]. This damage mode affects not only operating process, but also safety and economics as well. Therefore, it is necessary to find a good predictive method to accurately predict the erosion rate for offshore equipment.

The erosion mechanism is different in ductile and brittle materials. A number of studies have been performed to reveal the erosion mechanisms of ductile and brittle materials [2-6]. It is now known that brittle materials erode by cracking and chipping, while ductile materials erode by a sequence of micro-cutting, forging and fracture, etc [7]. Hence, erosion rate and mechanism are highly dependent on material types.

So far, several experimental methods have been developed to determine the eroded volume of a material. However, the experimental data found in the literature often refer to a particular material without specifying their properties and operating conditions. Therefore, the experimental erosion rate for the same material reported by different authors can differ greatly [8].

Numerical simulations, such as the Finite Element Method (FEM), have also been used to characterize erosion wear. Previously, 2D models were mainly used to investigate the influencing parameters of erosion wear. However, 2D simulation cannot correctly consider the effects of multi-particle erosion. Hence, 3D FEM models have been often used to study the erosion process. For example, Alman et al. [9] studied erosion behavior of both brittle and ductile materials, and concluded that the impact angle is important for erosion mechanism: A ductile material exhibits the maximum erosion rate at an impact angle of about 20-40°, while a brittle material shows the maximum erosion rate at an impact angle of 90°. ElTobgy et al. [6] studied erosion wear process using multiple impacts with perfect spherical particles, and pointed out that single-particle impact is insufficient, and three or more particles are needed to simulate the erosion process. Subsequently, Wang et al. [7] performed finite element simulations on erosion wear with 100 sphere particles and analyzed the erosion rate of both ductile and brittle materials, and compared their simulation results with that using other computational models.

In this study, we perform three-dimensional FEM simulations using the Johnson-Cook models to study the erosion rate for multiple impacts with both spherical and non-spherical solid particles on a deformable substrate. The main objective is to analyze the erosion rate of different particles with

different impact angles and velocities, and compare the present simulation results with that using other computational and theoretical models.

## 2. Modeling

### 2.1. Material model

#### 2.1.1 General property

The erosion process has been studied widely using numerical approaches such as finite element method. One key point in simulation is the choice of material model considering strain, strain rate and temperature. To study erosion process, a model must have three important components: elasticity, plasticity, damage initiation and damage growth. In this study, the substrate material is Ti-6Al-4V, and elastic response of the material is assumed to be linear and defined by elastic modulus and Poisson's ratio. Thermal response is ignored because of transient process.

#### 2.1.2. Plasticity model

The Johnson-Cook visco-plastic model (J-C) is used in this study [10, 11]. In this model, flow stress  $\bar{\sigma}$  depends on equivalent plastic strain ( $\bar{\epsilon}$ ), equivalent plastic strain rate ( $\dot{\bar{\epsilon}}$ ), and temperature. The model can be expressed as follows:

$$\bar{\sigma} = (A + B\bar{\epsilon}^n) \left( 1 + C \ln \left( \frac{\dot{\bar{\epsilon}}}{\dot{\bar{\epsilon}}_0} \right) \right) (1 - T^{*m}), \quad (1)$$

where  $A$ ,  $B$ ,  $C$  and  $m$  are material constants,  $n$  is strain hardening exponent,  $\dot{\bar{\epsilon}}/\dot{\bar{\epsilon}}_0$  is the normalized equivalent plastic strain rate (typically normalized by a strain rate of  $1.0 \text{ s}^{-1}$ ), and  $T^*$  is the homologous temperature which is defined as:

$$T^* = \frac{T - T_r}{T_m - T_r}, \quad (2)$$

where  $T$  is the current temperature,  $T_r$  is the reference temperature,  $T_m$  is the melting temperature of material. The model assumes that strength is isotropic.

#### 2.1.3. Failure model

Johnson-Cook failure model is applied for the ductile failure criterion [10, 11], in which the equivalent plastic strain at the onset of damage,  $\bar{\epsilon}_D^{pl}$ , is assumed to be a function of stress triaxiality ( $\eta$ ), strain rate ( $\dot{\epsilon}^*$ ) and temperature. Johnson-Cook damage model is expressed in term of the failure strain as follows:

$$\bar{\epsilon}_D^{pl} = [d_1 + d_2 \exp(-d_3 \eta)] (1 + d_4 \ln \dot{\epsilon}^*) (1 + d_5 T^*), \quad \eta = \frac{p}{q} \quad (3)$$

where  $d_1 - d_5$  are material constants,  $p$  is the pressure stress (positive in tension),  $q$  is the von-Mises stress, and  $T^*$  is the homologous temperature.

In the explicit finite element method, the overall damage variable  $D$  captures the combined effects of all active damage mechanisms, and is computed in terms of the individual damage variables. The damage parameter  $D$  is defined as:

$$D = \frac{\sum \Delta \epsilon^{pl}}{\bar{\epsilon}_D^{pl}} \quad (4)$$

In each finite element,  $(\sum \Delta \epsilon^{pl})_i$  is calculated, and the damage parameter  $D$  for element  $i$  is subsequently calculated during each time step. When the damage parameter  $D$  reaches the value of

1, the element  $i$  is assumed to have failed and removed from the model instantly [7].

#### 2.1.4. Equation of state

When a ductile material is impacted by erodent particles at a considerably high speed, the Grüneisen equation of state (EOS) [7] is used to simulate the shockwave effects for ductile material. The shockwave velocity  $v_s$  is much higher than the elastic-plastic wave or material velocity. Across the shock wave, a discontinuity takes place in material properties. The cubic shock velocity  $v_s$  and material particle velocity  $v_p$  obey the following relation:

$$v_s = C_0 + Sv_p \quad (5)$$

Table 1. Material constants of Ti-6Al-4V

Material properties	Symbol	Ti-6Al-4V
Density	$\rho$ (kg/m <sup>3</sup> )	4428
Elastic modulus	$E$ (GPa)	113.8
Poisson's ratio	$\nu$	0.31
J-C yield strength	$A$ (MPa)	1098
J-C hardening coefficient	$B$ (MPa)	1092
J-C strain hardening exponent	$n$	0.93
J-C strain rate constant	$C$	0.014
J-C softening exponent	$m$	1.1
Melting temperature	$T_m$ (K)	1878
J-C damage constant	$d_1$	-0.09
J-C damage constant	$d_2$	0.27
J-C damage constant	$d_3$	0.48
J-C damage constant	$d_4$	0.014
J-C damage constant	$d_5$	3.87
Elastic bulk wave velocity	$C_0$ (km/s)	5.13
Slope in $v_s$ vs. $v_p$ diagram	$S$	1.028
Grüneisen coefficient	$\gamma_0$	1.23

where  $C_0$  is the elastic bulk wave velocity. For compressed materials ( $\mu > 0$ ), the pressure is defined as follows:

$$P = \frac{\rho_0 C_0^2 \mu [1 + (1 - \gamma_0/2)\mu - (a/2)\mu^2]}{[1 - (S-1)\mu]^2} + \gamma_0 E, \quad (6)$$

For expanded materials ( $\mu < 0$ ), the pressure is defined as follows:

$$P = \rho_0 C_0^2 \mu + (\gamma_0 + a\mu)E_0 \quad (7)$$

where  $\gamma_0$  is the Grüneisen gamma,  $a$  is the first-order volume correction to  $\gamma_0$ , and  $\mu = \rho/\rho_0 - 1$ ,  $\rho$  is for current density, and  $\rho_0$  is initial density. The material constants for Ti-6Al-4V are listed in [Table 1. Table 1](#) [6].

## 2.2. FE model

The erosion wear process is simulated using a commercial finite element solver, ABAQUS/Explicit (Version 6.11-2). The analysis is performed using Lagrangian formulation. In previous study,

ElTobgy et al. [6] reported that single particle impact is insufficient to simulate the erosion process, three and more particles are needed to analyze multiple particle interactions. In this study, 5 particles are used to ensure the accuracy of the model. In general, the erosion rate (%) is used to describe the erosion wear performance of the substrate material. Our objective is to analyze the material erosion rate under various processing conditions. The erosion rate is defined as [7]:

$$\text{erosion rate} = \frac{\text{cumulative mass loss of substrate material}}{\text{impact particles weight}} \quad (8)$$

### 2.2.1. Impact particle

Two kinds of impact particle are used in the present simulation study, that is, spherical and irregular non-spherical particles. The purpose is to consider the effect of particle shape on material removal mechanism. The impacting material is steel with a density of  $7800 \text{ kg/m}^3$ . In the finite element model, the impact particle material is modeled as a rigid body. The element for the impact particle is 3-node and 4-node bilinear quadrilateral rigid elements (R3D3 and R3D4).

### 2.2.2. Impact substrate

The substrate is modeled as a deformable elastic plastic material, and the eight-node brick hexahedral element with reduced integration and hourglass control (C3D8R) is used to mesh the substrate. The accuracy of the material removal prediction is tested with different grid sizes for convergence test. In this study, mesh size is chosen to ensure neither time-consuming nor leading to unreasonable discrepancy. Figures 1 and 2 show the FE model of spherical and irregular particles. General contact is defined between the impacting particles and substrate material. The contact property is assumed to follow coulomb friction, and the friction coefficient between impact particle and substrate is assumed to be 0.2 [12], the boundary condition is applied to ensure that the substrate is fixed for bottom plane and the particles rotation are constrained in all three directions.

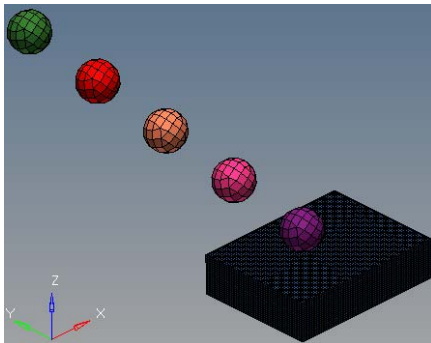


Figure 1. Spherical particle FE model

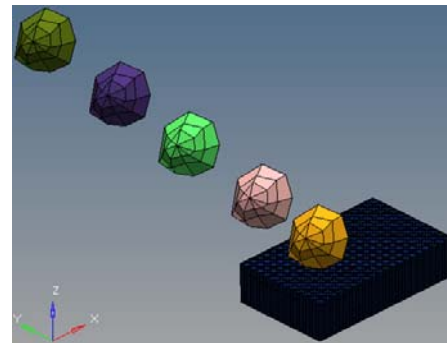


Figure 2. Irregular particle FE model

When particles impact the substrate, some of impacts, depending on the impact velocity and angle, will only deform the material surface without causing material removal, leading to the hardening of substrate material. In the previous attempts of erosion wear process simulation, most of them do not consider such hardening effect. In practice, the influence of multi-particle impacts is obvious in erosion process since the impact contact may change after multiple impacts. Therefore, although ideal cases, in which particle impacts with the same velocity and angle are employed, it is still necessary to adopt the multiple particle impact model. Figure 3 shows the material removal after each spherical particle impact. It clearly shows that the material removal increases with increasing impact times under the same impact condition.

ElTobgy et al. [6] showed that the erosion rate is affected by a number of system parameters, such

as particle velocity and impact angle, etc. Here we would like to calculate the erosion rates for various cases with a velocity range of 70-130m/s (10m/s interval) and an angle range of 20-75°. In addition, ElTobgy et al. [6] also pointed out that the sphere sizes have no obvious influence on erosion rate. Therefore in the present paper, we fix the sphere size, that is, the volume of the irregular impact particle is chosen to have the same volume as the spherical one with a diameter of 1mm. The same velocity and angle ranges for both spherical and irregular particles are used in the present study. The detailed analysis will be presented in the next section.

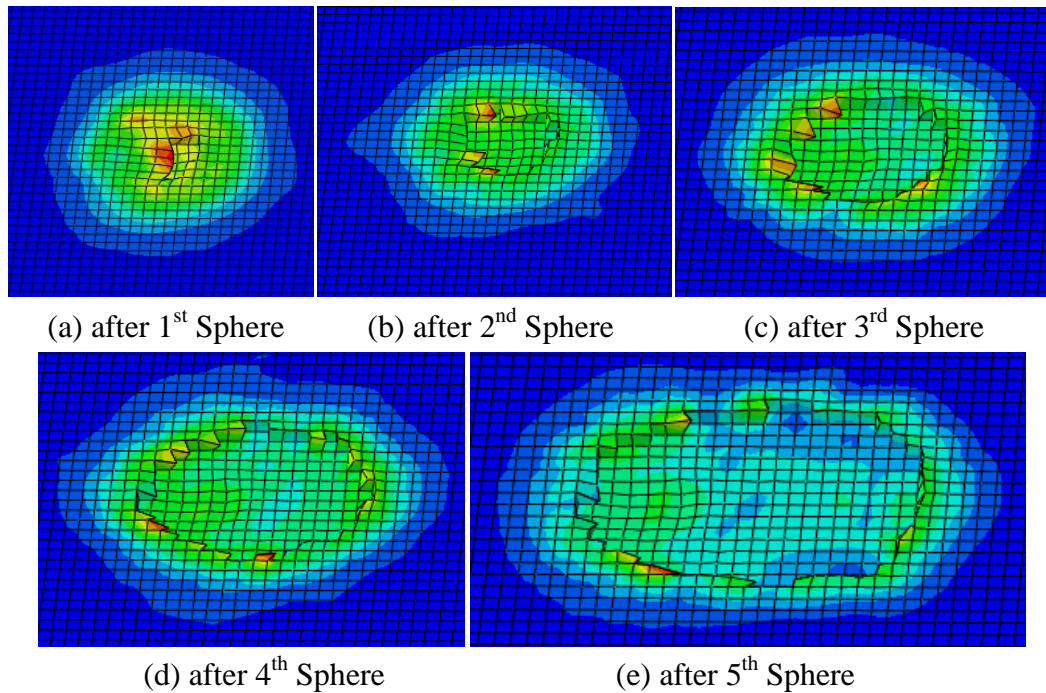


Figure 3. Material removal for 5 particle impacts sequentially (velocity =100m/s, angle = 30°)

### 3. Results and discussion

#### 3.1. Effect of impact velocity on erosion rate

To calculate the erosion rate, we perform FE simulations on the impact of spherical particles at an impact angle of 45° and different velocities using the same substrate and impacting material. Table 2 shows the cumulative mass loss of substrate material after each sphere impact. It is seen that when the velocity is low, no material removal occurs or mass loss is relatively small. When the impact velocity is high, however, more mass loss occurs and in some cases, the penetration occurs after several particle impacts.

Table 2. Cumulative mass loss of the substrate material ( $10^{-6}$ kg)

Angle	Velocity (m/s)	1 <sup>st</sup> Sphere	2 <sup>nd</sup> Sphere	3 <sup>rd</sup> Sphere	4 <sup>th</sup> Sphere	5 <sup>th</sup> Sphere
45°	70	0	0	0	1.10E-03	6.70E-03
	80	0	0	5.60E-03	2.66E-02	5.37E-02
	90	0	3.90E-03	3.10E-02	7.20E-02	1.16E-01
	100	0	1.44E-02	6.53E-02	1.20E-01	1.78E-01
	110	5.00E-04	3.60E-02	9.96E-02	1.68E-01	penetration
	120	5.50E-03	5.86E-02	1.44E-01	penetration	
	130	1.55E-02	9.91E-02	2.08E-01	penetration	

Figure 4 shows cumulative mass loss of the substrate material after 5 sphere particle impacts. It is seen that the material removal is very small after the first impact and then increases with the number of impacts. In some cases, impact particles are able to penetrate into the substrate, which is not included in the cumulative mass loss.

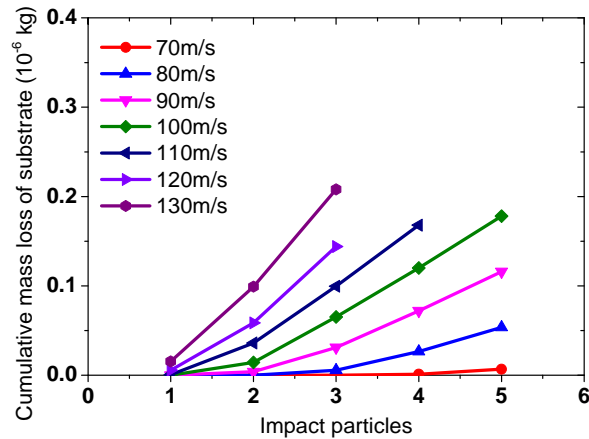


Figure 4. Variation of cumulative substrate mass loss

As defined in the above section, erosion rate is the ratio of the cumulative mass loss of the substrate and the weight of impact particles. The relationship between erosion rate and impact velocity was proposed following a power law function from publications [13 - 16], that is,

$$\text{erosion rate} \propto V^n \quad (9)$$

However, the exponent value  $n$  differs with different literatures. Finnie [13] proposed the exponent of 2 and Hashish [14] gave a value of 2.5, respectively. Scheldon et al. [15] experimentally obtained an exponent value in the range of 2-3, while Yerramareddy et al. [16] reported a value of 2.35 for Ti-6Al-4V. In general, the exponent value  $n$  is in the range of 2.0 - 2.7. For metallic material, the value is in the range of 2.0 - 2.5 [6, 7].

Figure 5 shows the relation of erosion rate with the impact velocities in log - log scale. The slope of linear fitting curve gives an exponent value  $n$  equal to 2.22 for Ti-6Al-4V, which is in accordance with the range reported by other researchers [13-16]. In addition, ElTobgy et al. [6] explained the reason for the relation between velocity and erosion rate in terms of energy aspect.

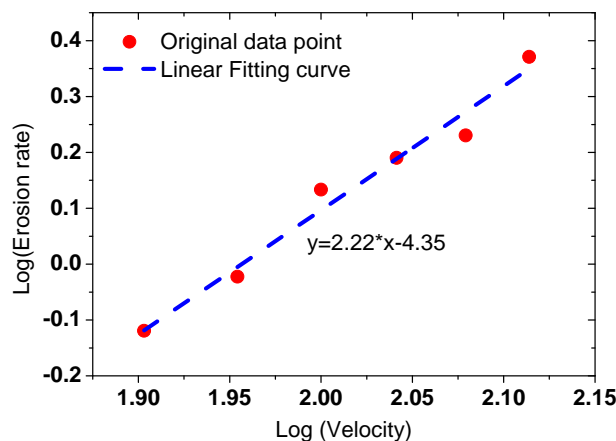


Figure 5. Erosion rate vs. velocity in log-log scale

Similarly, the relations between erosion rate and impact velocity have also been analyzed with irregular non-spherical particles. Figure 6 shows erosion rate and velocity relationship in log-log scale. The exponent value provided by the slope of linear fitting curve is 2.40, which is also in the

reported range [13-16]. However, the simulated exponent for irregular particles is higher than that for spherical particles. It can be explained from energy conversion. It is known that the kinetic energy is transformed into strain energy during impact. In this irregular non-spherical impact case, more kinetic energy is transformed into strain energy, resulting in more wear damage. Hence, at the same velocity, the erosion rate of the substrate material under irregular particle impacting is higher than that under spherical particle impacting. It will be interesting to investigate material removal with different particle geometries (cubic, tetrahedron, pentahedron, etc) in the future work, and study the relationship between erosion rate and geometry.

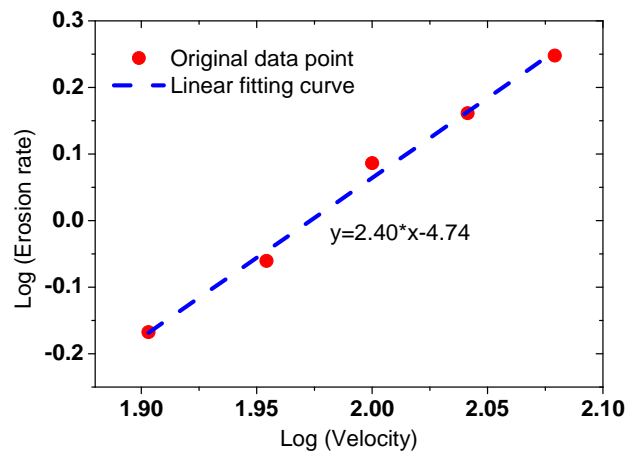


Figure 6. Erosion rate vs. velocity in Log-Log scale

### 3.2. Effect of impact Angle on erosion rate

Impact angle is also an important parameter influencing solid particle erosion. It was reported that the maximum erosion rate angle is a function of substrate material and is independent of erodent material properties [17]. Figures 7 and 8 show the relation between erosion rate and impact angle at velocities of 100m/s and 80m/s, respectively. Clearly, at the two different impact velocities, the two patterns are very similar, with the maximum erosion rate for both cases occurring at angle of 40-45°. ElTobgy et al. [6] obtained peak erosion rate at a 40° angle for Ti-6Al-4V, Wang et al. [7] reported maximum erosion rate at about 30° for the same substrate material, while Yerramareddy et al. [16] experimentally determined the maximum erosion rate occurs at an angle of 35-40°. Hence, the ranges of maximum erosion rate predicted from our finite element model are close to that from these literature data.

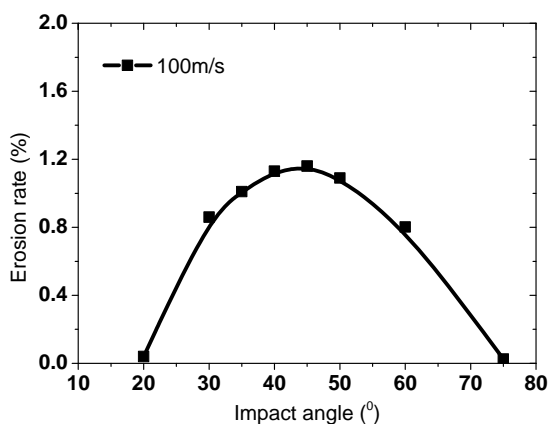


Figure 7. Erosion rate vs. velocity (v=100m/s)

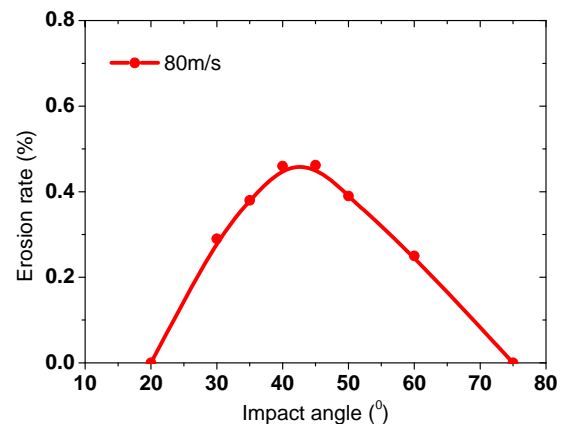


Figure 8. Erosion rate vs. velocity (v=80m/s)

## 4. Conclusions

We have performed FE simulations to study the erosion rate of a deformable substrate under multiple impacts using both spherical and irregular non-spherical solid particles. The material model employed is Johnson-Cook visco-plastic model for plastic deformation and Johnson-Cook material failure criterion for material removal. A five-particle impact process is employed to analyze the erosion process. The relations between the erosion rate and the impact angle and velocity have been obtained and compared with literature data. It is found that the erosion rate and velocity obey a power law relation and the exponent value obtained from our finite element simulation is in accordance with the literature ones. The exponent for irregular particles is higher than that for regular sphere particles. The impact angle for the maximum erosion rate predicted from our finite element simulation is in the range of 40–45°. This range agrees well with the published data. Interesting future research works include the establishment of the relation between material removal and particle geometry and the application of the model to study the erosion processes in complex offshore structures.

## References

- [1] Keles, Ozgul and Inal, O.T., A Review on Solid Particle Erosion of Ductile and Brittle Materials, *Recent Res. Devel. Mat. Sci.* 3, (2002) 499–528.
- [2] I. Finnie, Erosion of surfaces by solid particles. *Wear*, 3 (1960) 87–103.
- [3] J.G.A. Bitter, A study of erosion phenomena. Part I, *Wear*, 6 (1963) 5–21.
- [4] J.G.A. Bitter, A study of erosion phenomena. Part II, *Wear*, 6 (1963) 169–190.
- [5] I.M. Hutchings, Ductile–brittle transitions and wear maps for the erosion and abrasion of brittle materials. *J. Phys. D: Appl. Phys.* 25 (1992) A212–A221.
- [6] M.S. ElTobgy, E. Ng, M.A. Elbestawi., Finite element modeling of erosive wear. *International Journal of Machine Tools & Manufacture*, 45 (2005) 1337–1346.
- [7] Yu-Fei Wang, Zhen-Guo Yang., Finite element model of erosive wear on ductile and brittle materials. *Wear*, 265 (2008) 871–878.
- [8] D. Aquaro, E. Fontani, Erosion of Ductile and Brittle Materials, *Meccanica*, 36 (2001) 651–661.
- [9] D. Alman, J. Tylczak, J. Hawk, M. Hebsur, Solid particle erosion behavior of an Si<sub>3</sub>N<sub>4</sub>–MoSi<sub>2</sub>. *Mater. Sci. Eng.* A261 (1999) 245–251.
- [10] G.R. Johnson, W.H. Cook, A constitutive model and data for metals subjected to large strains, high strain rates and high temperatures, in: *Proceedings of the 7th International Symposium on Ballistics*, The Hague, 1983, pp.541–547.
- [11] G.R. Johnson, W.H. Cook, Fracture characteristics of three metals subjected to various strains, strain rates, temperatures and pressures. *Eng. Fract. Mech.* 21 (1) (1985) 31–48.
- [12] M. Meo, R. Vignovic, Finite element analysis of residual stress induced by shot peening process. *Adv. Eng. Software*, 34 (2003) 569–575.
- [13] I. Finnie, The mechanism of erosion of ductile metals. *Proceedings of the Third National Congress on Applied Mechanics*, New York, 1958, pp. 527–532.
- [14] M. Hashish, Modified model for erosion, *Seventh International Conference on Erosion by Liquid and Solid Impact*. Cambridge, England, 1987, pp. 461–480.
- [15] G.L. Sheldon, A. Kanhere, An investigation of impingement erosion using single particles. *Wear*, 21 (1972) 195–209.
- [16] S. Yerramareddy, S. Bahadur, Effect of operational variables, microstructure and mechanical properties on the erosion of Ti–6Al–4V. *Wear*, 142 (1991) 253–263.
- [17] G.R. Desale, B.K. Gandhi, S.C. Jain, Effect of erodent properties on erosion wear of ductile type materials. *Wear*, 261 (2006) 914–921.